

AD-A113 352

EASTERN ENTERPRISES BOULDER CO
A TWO-POINT CORRELATION STUDY OF INTERPLANETARY CONDITIONS AS O--ETC(U)
FEB 82 T YEH

F/6 3/2

NA60-RA-C-00103

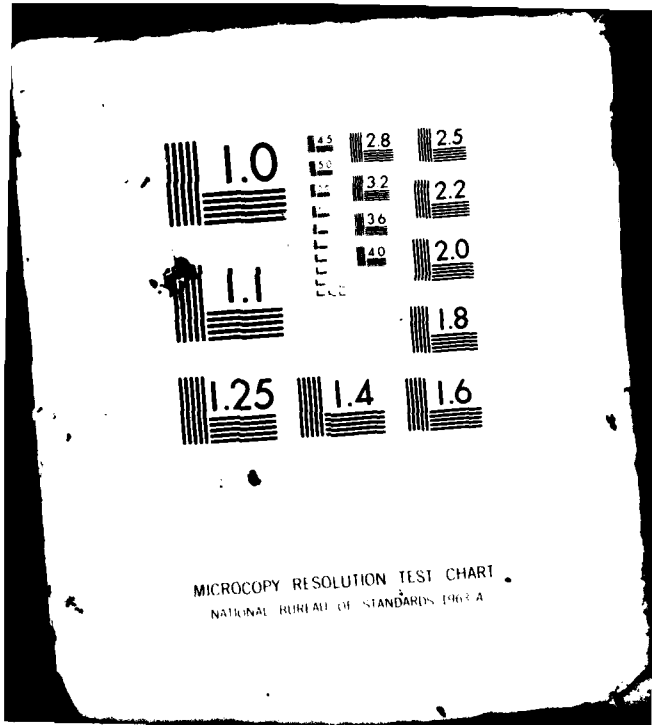
AFGL-TR-82-0073

NL

UNCLASSIFIED

1 x 1
A
1 300

END
DATE
FILED
5 82
DTB



AD A113352

ANGL-TR-62-0073

A TWO-POINT CORRELATION STUDY OF
INTERPLANETARY CONDITIONS AS OBSERVED
BY PIONEER 12 AND IMP 8

Tyan Yeh

Eastern Enterprises
4475 Ludlow Street
Boulder, Colorado 80303

Final Report
January 1980 - September 1981

February 1982

Approved for public release; distribution unlimited

AIR FORCE GEOPHYSICS LABORATORY
AIR FORCE SYSTEMS COMMAND
UNITED STATES AIR FORCE
HANSOM AFB, MASSACHUSETTS 01751

REF ID:
A113352

Unclassified

SECURITY CLASSIFICATION OF THIS PAGE (When Data Entered)

REPORT DOCUMENTATION PAGE		READ INSTRUCTIONS BEFORE COMPLETING FORM
1. REPORT NUMBER AFGL-TR-82-0073	2. GOVT ACCESSION NO. AIA/13352	3. RECIPIENT'S CATALOG NUMBER
4. TITLE (and Subtitle) A Two-point Correlation Study of Interplanetary Conditions as Observed by Pioneer 12 and IMP 8	5. TYPE OF REPORT & PERIOD COVERED Scientific - Final Jan 1980 - Sept 1981	6. PERFORMING ORG. REPORT NUMBER
7. AUTHOR(s) Tyan Yeh	8. CONTRACT OR GRANT NUMBER(s) Project Orders ESD 0-0918 and ESD 1-0858 to National Oceanic and Atmospheric Adm.	
9. PERFORMING ORGANIZATION NAME AND ADDRESS Eastern Enterprises 4475 Ludlow St. Boulder CO 80303	10. PROGRAM ELEMENT, PROJECT, TASK AREA & WORK UNIT NUMBERS 61102F Task 2311G1 CWU 2311G1AO	
11. CONTROLLING OFFICE NAME AND ADDRESS Air Force Geophysics Laboratory Hanscom AFB Massachusetts 01731 Monitor/M.A. Shea/PHG	12. REPORT DATE February 1982	13. NUMBER OF PAGES 32
14. MONITORING AGENCY NAME & ADDRESS (if different from Controlling Office)	15. SECURITY CLASS. (of this report) Unclassified	15a. DECLASSIFICATION/DOWNGRADING SCHEDULE
16. DISTRIBUTION STATEMENT (of this Report) Approved for public release; distribution unlimited		
17. DISTRIBUTION STATEMENT (of the abstract entered in Block 20, if different from Report)		
18. SUPPLEMENTARY NOTES Work performed through National Oceanic and Atmospheric Administration research contracts NA80RAC00103 and NA81RAA01021		
19. KEY WORDS (Continue on reverse side if necessary and identify by block number) Two-point correlation, Corotation, Solar wind streams, Pioneer 12, IMP 8		
20. ABSTRACT (Continue on reverse side if necessary and identify by block number) Correlations of interplanetary conditions at two interplanetary points are examined. Indirect comparisons are made between the observational data obtained by the Venus-bound space probe, Pioneer 12, and the Earth-bound satellite, IMP 8. The correspondence between the data points in the two sets of data is established by the assumption that solar wind streams corotate with the Sun. The streaming plasma in each stream tube is assumed to have a stationary profile under the effects of thermal conduction and solar gravitation.		

DD FORM 1 JAN 73 1473

Unclassified

SECURITY CLASSIFICATION OF THIS PAGE (When Data Entered)

1. Introduction

Many magnetospheric phenomena of the Earth are directly controlled by the solar wind which flows past the Earth. Thus, accurate prediction of the interplanetary conditions of the Earth is a prerequisite for a workable forecast of the magnetospheric dynamics of the Earth.

The interplanetary space is permeated by the solar wind which is continually emitted from the Sun. Hence, the interplanetary conditions evolve as the coronal conditions undergo changes. Although the solar wind is causally determined by what is present at the solar surface, the relationship between the interplanetary conditions of the Earth and the coronal conditions of the Sun is too complicated to allow a workable prediction of the former on the basis of a structureless description of the latter. The complication results from the spatial variations as well as the temporal evolutions over the solar surface. Evidently, the relationship between the conditions at two interplanetary points linked by a solar wind stream is much simpler. This is so, for in the far region of the interplanetary space energy deposition by means of processes other than thermal conduction is insignificant. Moreover, most of the stream-stream interactions take place before the solar wind reaches the far region. Therefore, prediction of conditions at one interplanetary point on the basis of conditions at another interplanetary point is more likely to be workable.

As a part of STIP (Studies of Travelling Interplanetary Phenomena) program, we undertake a two-point correlation study to explore the feasibility of a prediction scheme. First, we elucidate the theoretical solutions that represent the solar wind streams in the far region of the interplanetary space. Then, we present a useful approximation for the explicit expressions of these solutions. Such an approximation provides an efficient algorithm

for routine calculation of the solar wind streams. Finally, we use the observational data from the Venus-bound space probe Pioneer 12 and the Earth-bound satellite IMP 8, in conjunction with the solutions from theoretical modelling, to discern the two-point correlation in the interplanetary conditions. Such an assessment, aimed to ascertain the feasibility of the prediction of the Earth's interplanetary conditions, is possible with the recent availability of simultaneous data at 0.7 AU (where Pioneer 12 was inserted into Venus' orbit in December 1978) and 1.0 AU (where IMP 8 was launched into a geocentric orbit in October 1973).

Accession For	
NTIS GRA&I	<input checked="" type="checkbox"/>
DTIC TAB	<input type="checkbox"/>
Unannounced	<input type="checkbox"/>
Justification	
By _____	
Distribution/	
Availability Codes	
Dist	Avail and/or Special
A	



2. Governing Equations of Solar Wind Streams

As a starting point, we shall write the magnetohydrodynamic equations in a rotating frame of reference. Referring to a heliocentered spherical coordinates (r, θ, ϕ) which rotates at a constant angular velocity $\vec{\Omega} = \hat{z}\Omega_0$, the temporal and spatial variations of the physical quantities (viz, mass density ρ , temperature T , thermal pressure p , heating flux \vec{Q} , flow velocity \vec{u} , magnetic field \vec{B} , electric field \vec{E} , and current density \vec{J}) in rationalized units are governed by the following equations:

$$\frac{\partial}{\partial t} \vec{u} + \nabla \cdot \rho \vec{u} = 0 , \quad (1)$$

$$\rho \left(\frac{\partial}{\partial t} \vec{u} + (\vec{u} \cdot \nabla) \vec{u} + 2 \vec{J} \times \vec{x} \vec{u} - \vec{B}^2 \vec{q} \right) = -\nabla p + \rho \nabla \frac{GM_0}{r} + \vec{J} \times \vec{B} , \quad (2)$$

$$\frac{\partial}{\partial t} \rho \left(\frac{1}{2} \vec{u}^2 + \frac{3}{2} kT - \frac{1}{2} \vec{q}^2 + \frac{1}{2} \mu^{-1} \vec{B}^2 \right)$$

$$+ \nabla \cdot \left[\rho \left(\frac{1}{2} \vec{u}^2 + \frac{3}{2} kT - \frac{GM_0}{r} - \frac{1}{2} \vec{q}^2 \right) \vec{u} + p \vec{u} + \mu^{-1} \vec{E} \times \vec{B} + \vec{Q} \right] = 0 , \quad (3)$$

$$\frac{\partial}{\partial t} \vec{B} + \nabla \times \vec{E} = 0 , \quad (4)$$

$$\nabla \cdot \vec{B} = 0 , \quad (5)$$

in conjunction with the following relational equations

$$p = K \rho T , \quad (6)$$

$$\vec{J} = \mu^{-1} \nabla \times \vec{B} , \quad (7)$$

$$\vec{E} = - \vec{u} \times \vec{B} , \quad (8)$$

$$\vec{Q} = \frac{(-\kappa \nabla T) \cdot \vec{B}}{\vec{B}^2} \vec{B} . \quad (9)$$

The vector \vec{q} is the axial distance from the solar axis of rotation (viz. $q = r \sin \theta$). The constants G , M_\odot , K and μ are the gravitational constant, the solar mass, the gas constant (viz, Boltzmann constant divided by average mass of particles) and the magnetic permeability. The thermal conductivity $\kappa = C T^{5/2}$ depends on the temperature, with the coefficient C essentially constant.

We remark that the thermodynamic quantities ρ , T , p , Q as well as the magnetic field \vec{B} and current density \vec{J} are invariant in the coordinate transformation. In the rest frame the flow velocity is $\vec{u} + \Omega_\odot q \vec{l}_\phi$ and the electric field is $\vec{E} - \Omega_\odot q \vec{l}_\phi \times \vec{B}$, hence the kinetic energy is $\frac{1}{2} \vec{u}^2 + u_\phi \Omega_\odot q + \frac{1}{2} \Omega_\odot^2 q^2$ and the Poynting flux is $\mu^{-1} \vec{E} \times \vec{B} + (\Omega_\odot q \mu^{-1} \vec{B}^2) \vec{l}_\phi - (\Omega_\odot q \mu^{-1} B_\phi) \vec{B}$. The latter is clear if we recall that in a perfectly conducting medium the Poynting flux

$$\vec{E} \times \vec{B} = \left(\frac{1}{\mu} \mu^{-1} \vec{B}^2 \right) \vec{u} + \left[\left(\frac{1}{\mu} \mu^{-1} \vec{B}^2 \right) \vec{l}_\phi - \vec{B} \vec{B} \right] \cdot \vec{u} \quad (10)$$

consists of the convected flux of magnetic energy and the work done by the magnetic stress ($\hat{I}\hat{I}$ stands for the unit dyadic). Moreover, although spatial derivatives are invariant in the coordinate transformation, the temporal derivative in the rest frame is $\partial/\partial t - \Omega_0 \partial/\partial\phi$, hence an azimuthal variation in the rotating frame will appear as a temporal variation in the rest frame.

It is instructive to write the equation of azimuthal motion in the conservation form for angular momentum

$$\begin{aligned} \frac{\partial}{\partial t} (\alpha \rho u_\phi + \rho q^2 \Omega_0) + \nabla \cdot [(\alpha \rho u_\phi + \rho q^2 \Omega_0) \vec{u}] \\ = - \frac{\partial}{\partial \phi} p + \frac{1}{\mu} \mu^{-1} \vec{B}^2 + \nabla \cdot (\mu^{-1} q B_\phi \vec{B}) . \end{aligned} \quad (11)$$

The term $\partial/\partial t(\rho q^2 \Omega_0) + \nabla \cdot (\vec{u} \rho q^2 \Omega_0)$ accounts for the torque $2\rho \Omega_0 \vec{q} \cdot \vec{u}$ exerted by the Coriolis force and the term $\partial/\partial \phi p$ accounts for the torque exerted by the thermal pressure. Clearly, $q(pU_\phi + q\Omega_0)$ is the material angular momentum in the rest frame, and $(q^2 \mu^{-1} \vec{B}^2) \vec{I}_\phi - (\mu^{-1} q B_\phi) \vec{B}$ represents the flux of magnetic angular momentum. Also, it is instructive to write the equation of energy conservation in the form

$$\rho \left[\frac{\partial u}{\partial t} + u \cdot \nabla u \right] + \frac{1}{2} \rho u^2 + \frac{1}{2} \rho q^2 \Omega_0^2 + \frac{1}{\mu} \vec{B}^2 = - \nabla \cdot \vec{q} , \quad (12)$$

which expresses the increase of entropy $S = K \log(T^{3/2}/\rho)$ by the heating flux.

Now we consider a solar wind stream that appears time-independent and hydromagnetically aligned (i.e., the flow velocity is parallel to the magnetic field) in the rotating frame. Since, by equation (8), the electric field is zero, equation (4) is satisfied. Let ℓ be a length variable that increases outward (viz. away from the sun) along the axis of a flux tube. Hence, $\vec{B} = \pm \vec{i}_\ell B$ (with the positive sign if the field line's polarity is outward and the negative sign if inward), $\vec{u} = \vec{i}_\ell u$ and $\vec{Q} = \vec{i}_\ell Q$. Equation (9) means that the heat flux conducting along the flux tube has the magnitude

$$Q = - C T^{5/2} \frac{dT}{d\ell} . \quad (13)$$

By virtue of equation (5), the field strength B varies inversely with the cross-sectional area of the flux tube. Accordingly, equation (1) yields the invariance of the mass efflux

$$\dot{m} = \frac{\rho u}{B} \quad (14)$$

and equation (3) yields the invariance of the energy efflux

$$\dot{E} = \frac{\rho \left(\frac{1}{2} u^2 + \frac{5}{3} kT - \frac{GM_\odot}{r} - \frac{1}{2} \Omega_\odot^2 q^2 \right) u + Q}{B} \quad (15)$$

along the flux tube. Furthermore, if the azimuthal gradient of the hydromagnetic pressure is negligible, then equation (11) yields the invariance of the hydromagnetic angular momentum efflux

$$\mathcal{L} = \frac{\rho q (u_\phi + \Omega_0 q) u - \mu^{-1} q B_\phi B}{B} \quad (16)$$

along the flux tube.

In our exposition of solar wind streams along flux tubes that spiral on helioapexed poloidal cones, the equation of poloidal motion will not be used. The equation of radial motion can be written as

$$\frac{r du_r}{u_r dr} = \frac{(u_\phi + \Omega_0 r \sin \theta)^2 + KT(2 - \frac{r}{T} \frac{dT}{dr}) - \frac{GM_\odot}{r} + \frac{r}{\rho} J_\theta B_\phi}{u_r^2 - KT}, \quad (17)$$

in which $J_\theta = -\mu^{-1} r^{-1} d(rB_\phi)/dr$ is the poloidal current if the azimuthal gradient of B_r is negligible. The equation of longitudinal motion

$$\rho \left(u \frac{du}{dr} - u_\phi^2 - q \frac{dq}{dr} \right) = - \frac{dp}{dt} + \rho \frac{d}{dr} \frac{GM_\odot}{r} \quad (18)$$

can be combined with equation (15) to yield the entropy equation

$$\frac{d}{dr} \left[\frac{3}{2} KT + p \frac{d}{dr} \frac{1}{\rho} \right] = - \frac{d}{dr} \frac{Q}{\rho u} \quad , \quad (19)$$

which can also be obtained directly from equation (12).

3. Solutions for Spiraling Solar Wind Streams

In the far region of the interplanetary space, the flux tubes are likely to spiral on poloidal cones (viz, $\theta = \text{const.}$). This means $B_\theta = 0$. On the other hand, the magnetic field has an azimuthal component

$$B_\phi = \frac{\mu}{r \sin \theta} \frac{\ell - m \Omega_0 r^2 \sin^2 \theta}{\mu \frac{m}{\rho} - 1} . \quad (20)$$

This follows from equation (16) in conjunction with the kinematic relationship $u_\theta = B_\theta u/B$ implied by the alignment of the stream tube with the flux tube. In the absence of stream-stream interaction, the cross-sectional area of a flux tube will have its radial projection varying as r^2 . Accordingly, the invariance of the magnetic flux along a flux tube takes the form

$$\mathcal{F} = r^2 B \cos \chi \quad (21)$$

in which the spiral angle of the flux tube

$$\chi = \arctan \frac{B_\phi}{B_r} \quad (22)$$

is the angle between its axis and the heliocentric radial line. Next, in view of the kinematic relationship $u_r = B_r u/B$, it is seen that $r^2 \rho u_r$ is equal to $\mathcal{M} \mathcal{H}$. Upon the use of $dr/d\ell = \cos \chi$ and $\rho = M \mathcal{H} r^2 u_r$, equation (19) can be written as

$$\frac{d}{dr} \left(\frac{C}{K} \frac{\cos^2 \chi}{\mathcal{M} \mathcal{F}} r^2 T^{5/2} \frac{dT}{dr} \right) - \frac{3}{2} \frac{dT}{dr} - (2 + \lambda) \frac{T}{r} = 0 \quad , \quad (23)$$

in which $\lambda \equiv (r/u_r)(du_r/dr)$ is given by equation (17).

Now specification of ρ , u , T , B , and χ at an interplanetary point with radial distance r will determine the geometry of a spiraling flux tube passing through that point as well as the physical profile of the solar wind stream in that flux tube. The heat flux must take on a certain compatible value determined by the above-mentioned specified values, so that the pressure will vanish at infinity. Equations (13) and (23) constitute a second-order system of differential equations for T and Q . It determines two functional combinations which are invariant along the flux tube. One of these two invariants must take on a certain value (say, zero), thus providing the compatibility constraint which will determine the heat flux. The other invariant can take on an arbitrary value, say, ζ . We do not know the mathematical expressions nor the physical meanings of these two obscure invariants. At any rate, the six invariants (namely, \mathcal{W} , \mathcal{E} , \mathcal{L} , \mathcal{J} , ζ , and zero) will determine the six variables (namely, ρ , u , T , B , χ and Q) as functions of r . The difficulty lies in the judicious determination of the compatible heat flux in terms of the observed values of the remaining five quantities. Since this is a two-point boundary value problem, trial-and-error method of numerical shooting in conjunction with numerical integration of differential equations is rather tedious. In the next section we shall obtain analytic expressions which are satisfactory approximations for the compatibility constraint and the invariant ζ .

4. An Approximate Solution in Explicit Expressions

We have formulated a deterministic set of equations, whose solutions, satisfying the condition of vanishing pressure at infinity, will describe solar wind streams in the interplanetary space. The solutions of the differential equations (13) and (23) can be visualized as curves in the (r , T , Q) space. Not all solutions are physically admissible. The admissible solution should have the property that $T \rightarrow 0$ as $r \rightarrow \infty$. Some properties of the admissible solutions are clear from the invariants along a flux tube. First, the radial velocity attains a finite value at large heliocentric distances. This follows from the fact that its kinetic energy is converted from the finite amount of thermal energy and heating flux. Thus, the dimensionless ratio λ diminishes to zero. In fact, most of the radial acceleration takes place during the transonic transition which occurs in the corona before the solar wind reaches the interplanetary space. Secondly, the spiral angle of the flux tube approaches 90° at infinity. This follows from the variations that the radial field decreases like r^{-2} whereas the azimuthal field decreases only like r^{-1} . Indeed, χ is rather large and increases very slowly in the interplanetary space. This can be seen from the equation

$$\frac{\tan i}{\tan \chi_0} = \frac{r}{r_0} \frac{M \Omega_0 r^2 \sin^2 \theta - L}{M \Omega_0 r_0^2 \sin^2 \theta - L} \frac{\mu M r_0^2 u_0 \cos \chi_0 - J}{\mu M r^2 u \cos \chi - J}, \quad (24)$$

which indicates $\chi \approx \arctan(r/r_0 \tan \chi_0)$ in the interplanetary space where the radial velocity does not change much. We use subscript "0" for the interplanetary "base" at which data are specified.

It is reasonable to analyze the problem by approximating the slowly varying λ and χ in equation (23) with constants. The approximating values $\bar{\lambda}$ and $\bar{\chi}$ may be chosen as λ_0 and χ_0 at the specified interplanetary point. In terms of the three similarity variables (Yeh, 1971)

$$R = C r , \quad (25)$$

$$X = \frac{C}{K} \frac{\cos^2 \bar{\chi}}{m^7} r T^{5/2} , \quad (26)$$

$$Y = \frac{1}{\bar{\lambda}} \frac{\cos \bar{\chi}}{m^7} \frac{r^2 Q}{T} , \quad (27)$$

the approximated equation (23) can be split into two coupled first-order differential equations

$$\frac{dR}{R} = \frac{dX}{X - \frac{5}{2}Y} = \frac{dY}{\frac{Y}{X}(Y + \frac{3}{2}) - (2 + \bar{\lambda})} . \quad (28)$$

The left-hand equation is also a rewriting of equation (13). The right-hand equation does not involve R. This means that the two-parameter family of solution curves in the (R, X, Y) space have a one-parameter family of projections in the (X, Y) plane. Among the latter family is a special curve which represents the constraint between Q and T as well as r necessary for the pressure to become vanishing at infinity. Other solutions of the right-hand equation are unphysical, for the subsequent solutions of the left-hand equation have the defects that either the temperature or the heat flux becomes negative eventually. On the other hand, the left-hand equation is linear in R. This means that various solutions differ only in scaling. We have accounted for the scaling by the inclusion of the arbitrary constant C in the definition of R in equation (26).

It turns out that the physically meaningful solutions of equations (28) are represented by three curves, which emanate from the critical point $R_C = 0$, $X_C = \frac{35}{4} + \frac{25}{4}\bar{\lambda}$, $Y_C = \frac{7}{2} + \frac{5}{2}\bar{\lambda}$ of the differential equation (28) and recede to $R = \infty$. The one with $X > X_C$, $Y > Y_C$ has the asymptotic property that T diminishes like $r^{-2/7}$ for large r (Parker, 1964). The one with $X = X_C$, $Y = Y_C$ has T diminishing like $r^{-2/5}$ (Whang and Chang, 1965). The one with $X < X_C$, $Y < Y_C$ has T diminishing like $r^{-4/3}$ (Durney, 1971). These three curves will be collectively denoted by $X = h(R)$, $Y = k(R)$. Their other projections will be denoted by $Y = f(X)$ and $R = g(X)$. Clearly, $h(R)$ and $g(X)$ are inverse functions to each other, whereas $k(R)$ is the composite function of $f(X)$ by $h(R)$. Each of these four functions has three branches (see Figure 1).

The function $f(X)$ has the following power series representations

$$X \left[\frac{4}{3} + \frac{2}{3}\bar{\lambda} \right] + \sum_{n=1}^{\infty} f_n^- X^n \quad \text{for } 0 < X < X_C$$

$$f(X) = Y_C \quad \text{for } X = X_C \quad (29)$$

$$X \left[\frac{2}{7} + \left(\frac{11}{9} + \frac{7}{9}\bar{\lambda} \right) X^{-1} + \sum_{n=1}^{\infty} f_n^+ X^{-n} \right] \quad \text{for } X_C < X < \infty$$

The coefficients are given by the recurrence formulas (with $f_0^- = \frac{4}{3} + \frac{2}{3}\bar{\lambda}$, $f_0^+ = \frac{2}{7}$, $f_1^+ = \frac{11}{9} + \frac{7}{9}\bar{\lambda}$):

$$f_n^- = \frac{2}{3} f_{n-1}^- - \sum_{i=1}^{n-1} \frac{5i+7}{3} f_i^- f_{n-1-i}^-,$$

$$f_n^+ = \frac{7}{2n+7} - \frac{2}{3} f_{n-1}^+ + \sum_{i=1}^{n-1} \frac{2i-7}{3} f_i^+ f_{n-1-i}^+.$$

The two branches approach $X = X_c$, $Y = Y_c$ with the slope

$$\left. \frac{df}{dX} \right|_{X=X_c} = \frac{1 + 5\bar{\lambda} + (2801 + 3410\bar{\lambda} + 1025\bar{\lambda}^2)^{1/2}}{175 + 125\bar{\lambda}}$$

The function $g(X)$ has the following power series representations.

$$g(X) = \begin{cases} X^{-3/(7+5\bar{\lambda})} \left(1 + \sum_{n=1}^{\infty} g_n^- X^n \right) & \text{for } 0 < X < X_c \\ \text{indefinite} & \text{for } X = X_c \\ X^{7/7} \left(1 + \sum_{n=1}^{\infty} g_n^+ X^{-n} \right) & \text{for } X_c < X < \sigma \end{cases} \quad (30)$$

The coefficients are given by the recurrence formulas (with $g_0^- = 1$, $g_0^+ = 1$):

$$g_n^- = \frac{15}{(14 + 10\bar{\lambda})n} \sum_{i=0}^{n-1} \left(-i + \frac{3}{7 + 5\bar{\lambda}} \right) f_{n-i}^- g_i^- ,$$

$$g_n^+ = \frac{25}{4n} \sum_{i=0}^{n-1} \left(i - \frac{7}{2} \right) f_{n-i}^+ g_i^+ .$$

The two branches approach $R = 0$, $X = X_c$ in a manner like $|X - X_c|^\alpha$ with the exponent

$$\alpha = \frac{1}{1 - \frac{5}{2} \left. \frac{df}{dX} \right|_{X=X_c}}$$

being greater than unity.

The function $h(R)$ has the following power series representations

$$h(R) = \begin{cases} R^{-(7+5\bar{\lambda})/3} \left[1 + \sum_{n=1}^{\infty} h_n^- R^{-n(7+5\bar{\lambda})/3} \right] & \text{for } X < X_c \\ X_c & \text{for } X = X_c \\ R^{2/7} \left[1 + \left(\frac{35}{36} + \frac{245}{36}\bar{\lambda} \right) R^{-2/7} + \sum_{n=2}^{\infty} h_n^+ R^{-2n/7} \right] & \text{for } X > X_c \end{cases} \quad (31)$$

with the coefficients given by the recurrence formula (with $h_0^- = 1$, $h_0^+ = 1$,

$$h_1^+ = \frac{35}{36} + \frac{245}{36}\bar{\lambda}:$$

$$h_n^- = -\frac{2}{n} \sum_{i=0}^{n-1} \left(i + \frac{10+10\bar{\lambda}}{14+\bar{\lambda}} \right) \frac{(2n+3i)(7+5\bar{\lambda})+41+25\bar{\lambda}}{45} h_i^- h_{n-1-i}^-$$

$$h_n^+ = -\frac{1}{n(2n+7)} \left[\frac{7}{4}(6n-61-35\bar{\lambda}) h_{n-1}^+ + \sum_{i=1}^{n-1} \frac{1}{5}(2n+3i)(2i+5) h_i^+ h_{n-i}^+ \right].$$

The function $k(R)$ has the following power series representations:

$$k(R) = \begin{cases} R^{-(7+5\bar{\lambda})/3} \left[\left(\frac{4}{3} + \frac{2}{3}\bar{\lambda} \right) + \sum_{n=1}^{\infty} k_n^- R^{-n(7+5\bar{\lambda})/3} \right] & \text{for } Y < Y_c \\ Y_c & \text{for } Y = Y_c \\ R^{2/7} \left[\frac{2}{7} - \sum_{n=1}^{\infty} k_n^+ R^{-2n/7} \right] & \text{for } Y > Y_c \end{cases} \quad (32)$$

with the coefficients given by the recurrence formulas (with $k_0^- = \frac{4}{3} + \frac{2}{3}\bar{\lambda}$,

$$k_0^+ = \frac{2}{7}):$$

$$k_n^- = \frac{2}{15} \left[n(7+5\bar{\lambda}) + (10+5\bar{\lambda}) \right] h_n^-$$

$$k_n^+ = \frac{2}{55} (10n+5) h_n^+.$$

Now, in view of equation (27), the compatible heat flux is given by

$$Q \approx K \rho_o u T f\left(\frac{C}{K} \frac{T^{5/2}}{r \rho u} \cos \chi\right) , \quad (33)$$

and in view of equation (25), the additional invariant is given by

$$\zeta \approx \frac{1}{r} g\left(\frac{C}{K} \frac{T^{5/2}}{r \rho u} \cos \chi\right) . \quad (34)$$

With these results, the admissible solution can be calculated in terms of r_o , ρ_o , u_o , T_o , B_o , and χ_o in the following algorithm. First, determine the compatible heat flux:

$$X_o = \frac{C}{K} \frac{T_o^{5/2}}{r_o \rho_o u_o} \cos \chi_o ,$$

$$Y_o = f(X_o) ,$$

$$Q_o = K \rho_o u_o T_o Y_o .$$

Next, evaluate the invariants:

$$\mathcal{M} = \frac{\rho_o u_o}{B_o} ,$$

$$\mathcal{E} = \frac{\rho_o u_o}{B_o} \left(\frac{1}{2} u_o^2 - \frac{1}{2} \Omega_o^2 r_o^2 \sin^2 \theta - \frac{GM}{r_o} + \frac{5}{2} KT_o \right) + \frac{Q_o}{B_o} ,$$

$$\mathcal{L} = (r_o \sin \theta) \left[\frac{\rho_o u_o}{B_o} (u_o \sin \chi_o + \Omega_o r_o \sin \theta) - \mu^{-1} B_o \sin \chi_o \right] ,$$

$$\mathcal{F} = r_o^2 B_o \cos \chi_o ,$$

$$\zeta = \frac{1}{r_o} g(X_o) .$$

Then calculate the physical quantities at the heliocentric distance r of interest:

$$R = \zeta r ,$$

$$T = \left[\frac{K}{C} \frac{m \zeta}{\cos^2 \chi_0} \frac{h(R)}{r} \right]^{2/5} ,$$

$$u = z^{1/2} \left[\frac{\mathcal{E}}{m} + \frac{1}{2} \Omega_0^2 r^2 \sin^2 \theta + \frac{GM_0}{r} - \frac{5}{2} KT - KT k(R) \right]^{1/2} ,$$

$$\chi = \arctan' \left(\frac{r}{r_0} \tan \chi_0 \right) ,$$

$$B = \frac{\mathcal{F}}{r^2 \cos \chi} ,$$

$$\rho = \mathcal{U} \left(\frac{B}{u} \right) .$$

5. Two-point Relationship in Corotating Streams

Now we consider a corotating solar wind stream in the equatorial plane (viz, $\theta = 90^\circ$). In the rest frame, this spiraling flux tube rotates at the angular velocity $\Omega_e = 360^\circ/27$ days. Let t_V be the instant when this corotating stream sweeps through Venus. At that time, the earth is azimuthally ahead of Venus by an azimuthal angle given by $\phi_E - \phi_V$. We want to know the later instant t_E when the same stream will sweep through the earth. The cross-section (denoted by E' in Figure 2) of the corotating stream that sweeps through the earth is slightly azimuthally behind the cross-section that sweeps through Venus. The azimuthal angle between these two cross-sections, one has the heliocentric distance $r_V = 0.72$ AU and the other $r_E = 1.0$ AU is

$$\phi_V - \phi_{E'} = -\frac{\tan(-x_V)}{r_V} (r_E - r_V) , \quad (35)$$

in which x_V is the spiral angle of the flux tube at the heliocentric distance r_V . Equation (35) is obtained from the differential equation $rd\phi/dr = B_\phi/B_r$ for the field line together with the equation $B_\phi/B_r \approx (r/r_V) \tan x_V$ along the flux tube. Since the earth is revolving around the sun at the angular velocity $\Omega_E = 360^\circ/365$ days, the time delay $t_E - t_V$ is equal to $(\phi_E - \phi_{E'})/(\Omega_e - \Omega_E)$. Hence

$$t_E = t_V + \frac{\phi_E - \phi_V}{\Omega_\odot - \Omega_E} + \frac{r_E - r_V}{\Omega_\odot - \Omega_E} \frac{\tan(-x_V)}{r_V} . \quad (36)$$

Note that x_V is negative, for angles are reckoned positive in the eastward direction of the solar rotation.

Next, suppose that the observed solar wind data at Venus (as measured by the space probe Pioneer-Venus) have the mass density ρ_V , the bulk speed U_V , the temperature T_V , the magnetic strength B_V and the spiral angle χ_V . From the transformation $U_r = u \cos \chi$, $U_\phi = u \sin \chi + \Omega_\odot r$ between the flow velocity \vec{U} in the rest frame and the flow velocity \vec{u} in the corotating frame, the flow speed in the corotating frame is given by

$$u_V = \left(U_V^2 - \Omega_\odot^2 r_V^2 \cos^2 \chi_V \right)^{1/2} + \Omega_\odot r_V \sin(-\chi_V) . \quad (37)$$

Using the algorithm described in the previous section, we can calculate the mass density ρ_E , the flow speed u_E , the temperature T_E , the magnetic strength B_E , and the spiral angle χ_E , at the heliocentric distance r_E . The corresponding bulk speed in the rest frame is

$$U_E = \left(u_E^2 + \Omega_\odot^2 r_E u_E \sin^2 \chi_E + \Omega_\odot^2 r_E \right)^{1/2} . \quad (38)$$

These extrapolation values are to be compared with the observation values of the solar wind at the earth at the instant t_E given by equation (36). The results will indicate to what extent the apparent temporal variation in the interplanetary space is due to the effect of corotation. From such a study, we can infer the time scale in which the temporal effect due to the intrinsic short-period changes of coronal condition may be neglected. In the following section we shall present the results obtained from the comparison of the Pioneer-Venus data with the data of earth-bound satellite, based on the model described in this section.

6. Correlation Features in Observational Data

We use observational data of Pioneer 12 and IMP 8 for the period from January 1980 to June 1980 to examine the two-point correlation features due to corotation of the solar wind streams in the interplanetary space. During this period, Venus to which Pioneer 12 is bound was azimuthally behind the Earth to which IMP 8 is bound. The Earth-Sun-Venus angle decreased from 103° on January 1, 1980 to 0° on June 15, 1980. Subsequently, Venus became azimuthally ahead of the Earth, by 120° on December 31, 1980. An azimuthal separation of 1° amounts to one day for the delay time of the rotating stream tubes.

Typical values of solar wind speed, density and temperature observed by Pioneer 12 were published in digital format in Solar-Geophysical Data, Part I (NOAA, 1980), whereas variations of solar wind speed, density and temperature observed by IMP 8 were published in graphic format in Solar-Geophysical Data, Part II (NOAA, 1980). Each triplet of data from Pioneer 12 represents the property of a solar wind stream at 0.7 AU. We use equations in section 4, with $\tau = t$, to calculate the values of speed, density and temperature at 1.0 AU. We also calculate the delay time, using Equation (16). The extrapolated values of speed, density and temperature at delayed times were plotted as dots in Figure 3. The segmental curves in the figures display the observational data of IMP 8. Coincidence of the three dots representing the extrapolated triplet with the three curves would mean perfect correlation. Since the data by IMP 8 were not in digital format, the correlation feature is to be examined visually rather than to be assessed in quantitative manner.

7. Discussions and Conclusions

In this study we have examined the data from Pioneer 12 and IMP 8 to discern the corotational correlations between the two sets of data observed at different regions of the interplanetary space. A high correlation is expected when the solar wind is in a quasi-steady state. We compare theoretically extrapolated values from Pioneer 12 data with corresponding IMP 8 data. The correspondence is determined by the assumption that solar wind streams corotate with the Sun. The extrapolation is done through a suitable modeling for solar wind streams in the far region of the interplanetary space.

The data from Pioneer 12 and IMP 8 as published in Solar-Geophysical Data (NOAA, 1980) consist of the three values of the flow velocity, particle density and temperature for the proton species, together with the azimuthal separation angle between the Earth and Venus, at selected times. We use the standard one-fluid solar wind equations with thermal conduction to extrapolate the velocity, density and temperature at 1.0 AU from the observed values at 0.7 AU.

The model we have used for solar wind streams is capable of accounting for correlation features arising from corotation of solar wind streams alone. There are many physical factors in the model whose simple-minded treatment cause deviations from good correlation between theoretically derived quantities and observationally obtained quantities. Among them are non-steady coronal conditions and non-radial streamlines. Each of these two is beyond the present state of arts for remedy. This is so not only because of the mathematical complexities in any time-varying or global treatment, but also because of the observational lack of structured coronal conditions.

Generally speaking, better correlation between interplanetary

points is achieved when the azimuthal separation between them is small. This is expected, for the simple reason that less temporal changes in the coronal condition enter the solar wind streams in a shorter duration of delay time.

In the realistic interplanetary space, temporal changes are always present. It seems plausible to regard these temporal changes as a series of quasi-steady states. If so, the relevant question is: what is the time scale over which the averages behave like quasi-steady quantities. For the purpose of a prediction scheme, the time scale should increase as the azimuthal separation angle increases. When the time scale exceeds the characteristic time of the magnetospheric phenomena of interest, prediction no longer makes sense. To assess the time scale of acceptable correlation, it seems worthwhile to perform correlation study based on temporally averaged, with chosen time scales, data. The present study uses instantaneous values of the interplanetary conditions at Venus and at the Earth. With the efficient methodology and numerical code developed in this study, the suggested study should be an accomplishable task.

Acknowledgments:

This study was supported by the Air Force Geophysics Laboratory project orders ESD 0-0918 and ESD 1-0858, through NOAA research contracts NA80RAC00103 and NA81RAA01021.

REFERENCES

- Cuperman, S. Plasma fluid aspects of the solar wind, Space Sci. Rev. 26, 277, 1980.
- Durney, B. A new type of supersonic solution for the inviscid equations of the solar wind, Astrophys. J., 166, 669, 1971.
- Durney, B. Solar wind properties at the earth as predicted by one-fluid models, J. Geophys. Res., 77, 4042, 1972.
- Hartle, R. E., and P. A. Sturrock. Two-fluid model of the solar wind, Astrophys. J., 151, 1155, 1968.
- Holzer, T. E. Effects of rapidly diverging flow, heat addition, and momentum addition in the solar wind and stellar winds, J. Geophys. Res., 82, 23, 1977.
- Leer, E., and T. E. Holzer. Energy addition in the solar wind, J. Geophys. Res., 85, 4681, 1980.
- Mestel, L. Magnetic braking by a stellar wind, Mon. Not. R. Astr. Soc. 138, 359, 1968.
- Parker, E. N., Dynamics of the interplanetary gas and magnetic fields, Astrophys. J., 128, 664, 1958.
- Parker, E. N., Dynamical property of stellar coronas and stellar winds. II. Integration of the heat flow equation, Astrophys. J., 139, 93, 1964.
- Pneuman, G. W., and R. A. Kopp. Gas-magnetic field interaction in the solar corona, Solar Phys., 18, 258, 1971.
- Weber, E. J., and L. Davis, Jr. The angular momentum of the solar wind, Astrophys. J., 148, 217, 1967.
- Whang, Y. C., and C. C. Chang. An inviscid model of the solar wind, J. Geophys. Res., 70, 4175, 1965.
- Yeh, T. Temperature profile of solar winds, J. Geophys. Res., 76, 7508, 1971.

Figure Captions

Figure 1. Plots of the functions $f(X)$ and $g(X)$. They describe the (Y,X) projection and the (R,X) projection of the critical solution of equation (28) with $\bar{\lambda} = 0$.

Figure 2. A corotating solar wind stream in the equatorial plane. The stream flows along a flux tube emanating from the sun (denoted by S). It sweeps through Venus (denoted by V) at time t_V and through the earth (denoted by E) at a later time t_E . The flux tube has a spiral angle χ_V at the heliocentric distance r_V of Venus. The cross-section (denoted by E') sweeping through the earth has the heliocentric distance r_E of the earth and is behind the cross-section sweeping through Venus by an azimuthal angle $\phi_V - \phi_E$. The earth is ahead of Venus by an azimuthal angle $\phi_E - \phi_V$ at time t_V .

Figure 3. Time-sequence plots of the interplanetary conditions, indicated by particle density, flow speed and temperature, of the Earth. The dots depict the theoretical values extrapolated from the observational data of Pioneer 12, whereas the curves depict the observational data of IMP 8. The Earth-Sun-Venus angle is indicated on the top of panel.

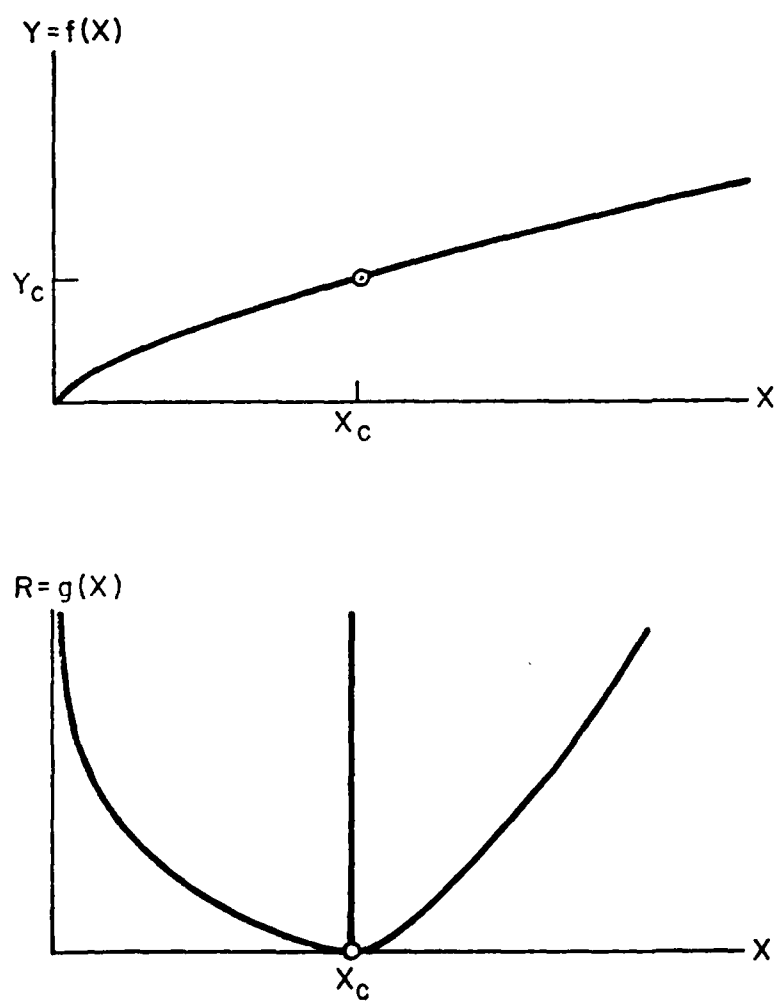


Figure 1

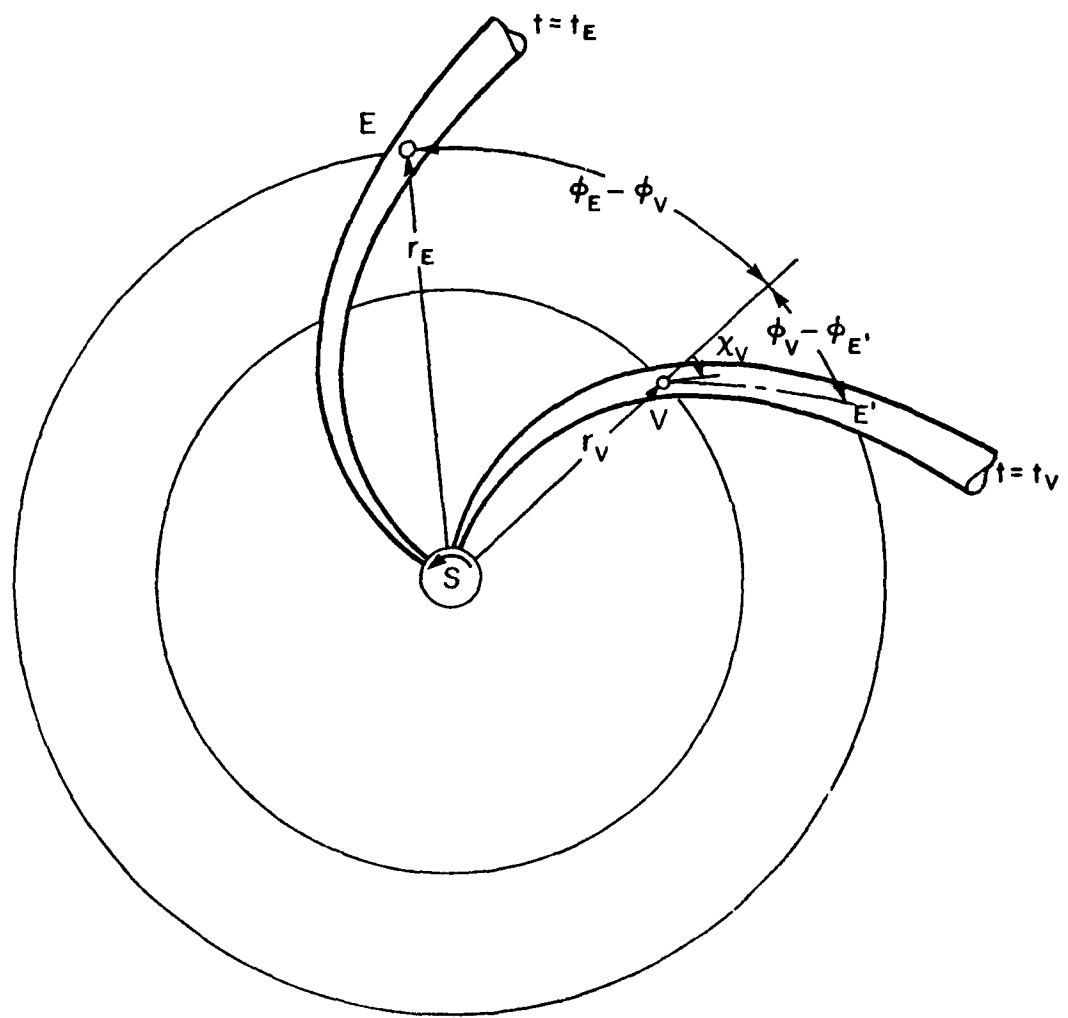


Figure 2

January 1980

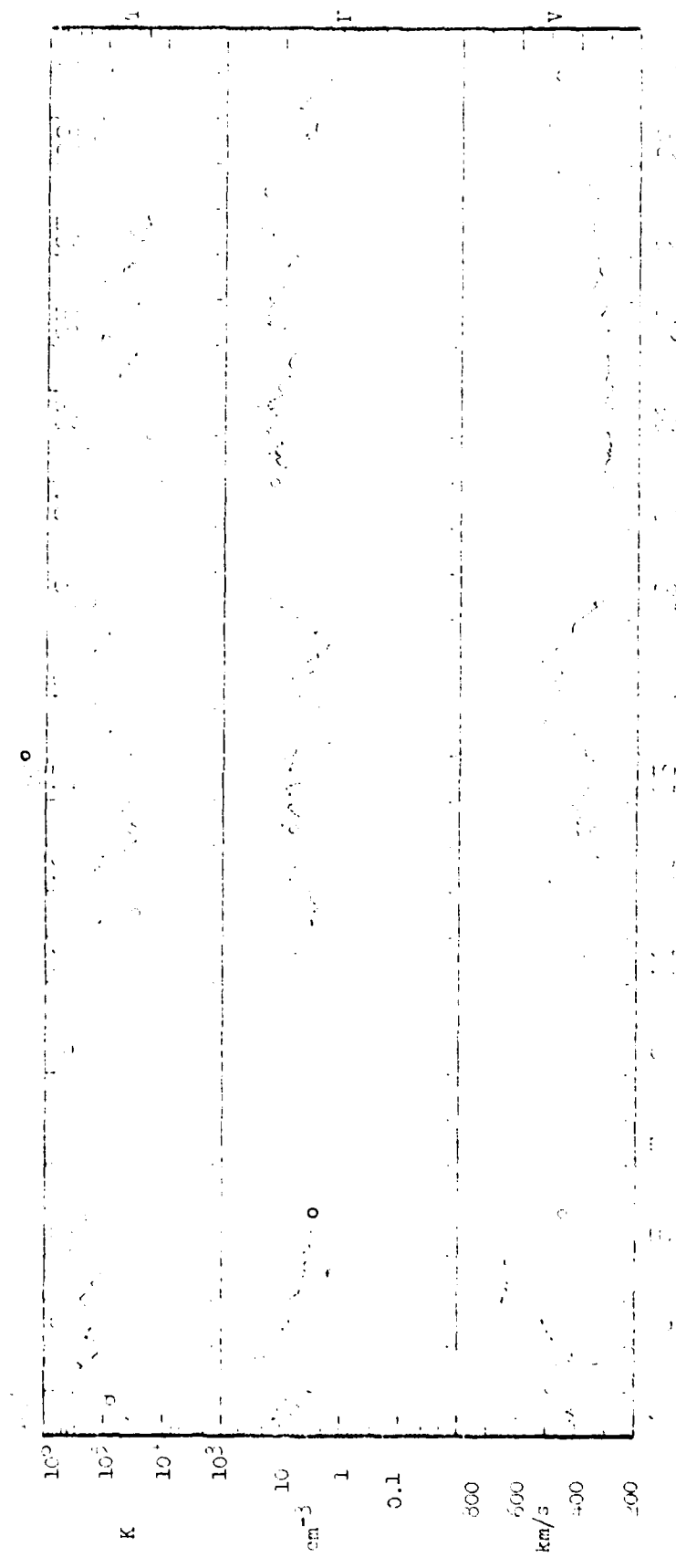


Figure 15

February 1980

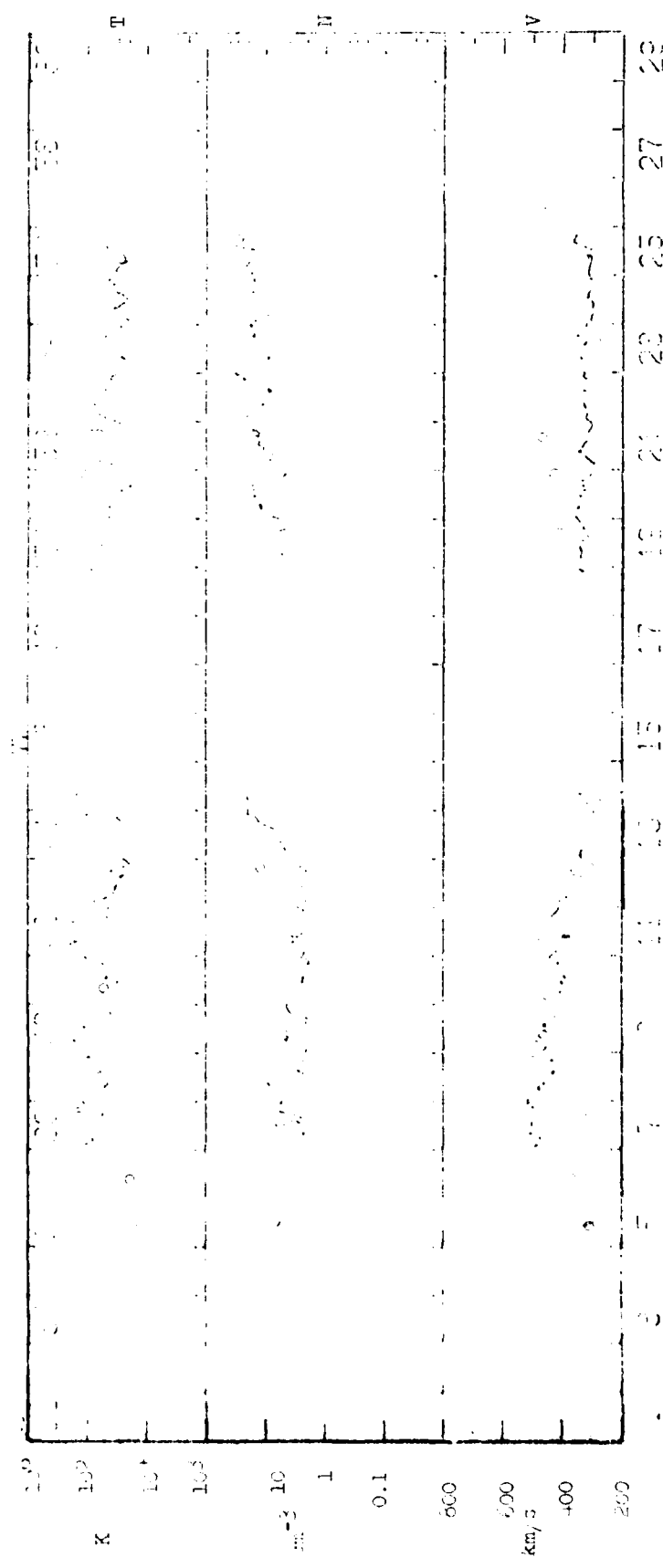
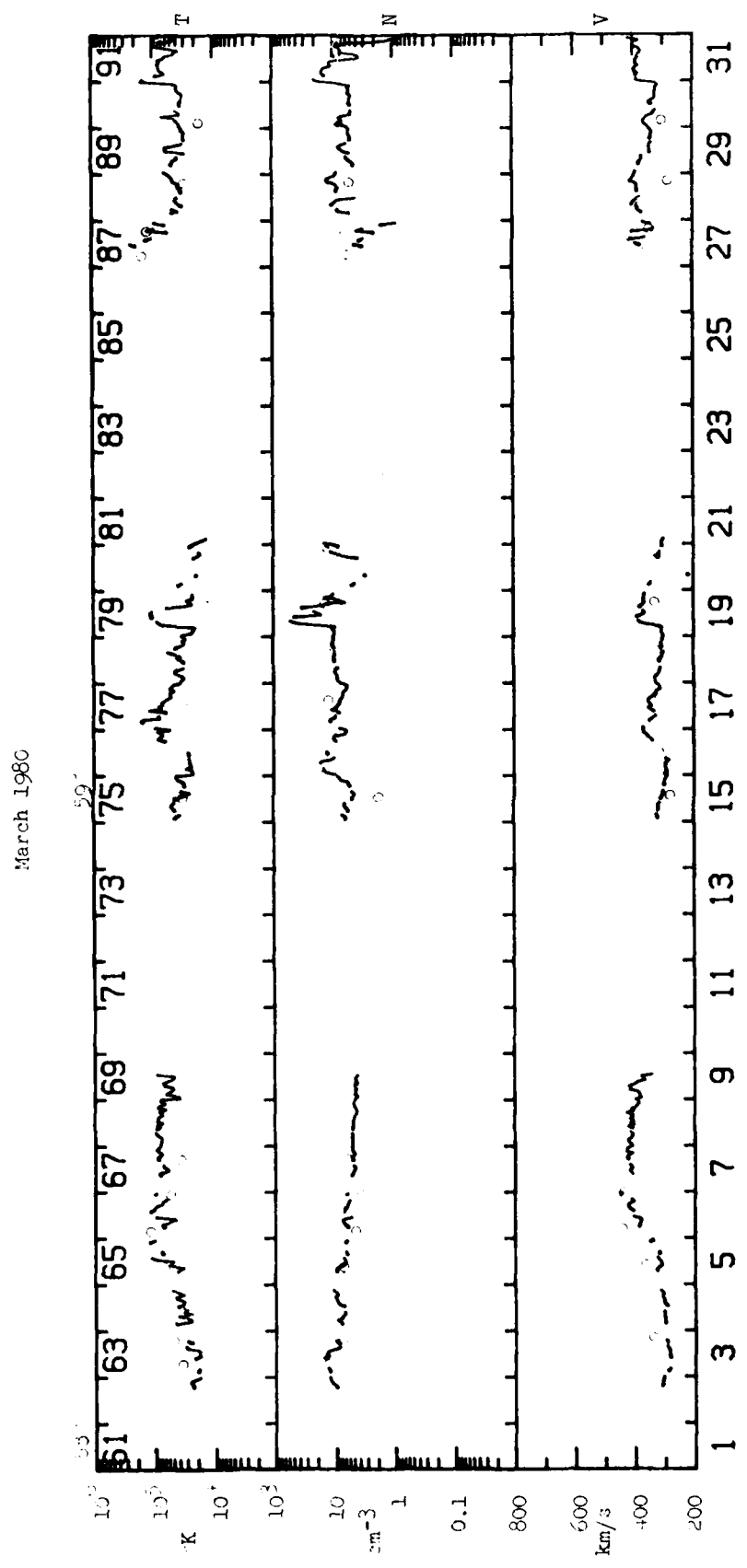


Figure 30



卷之三

April 1980

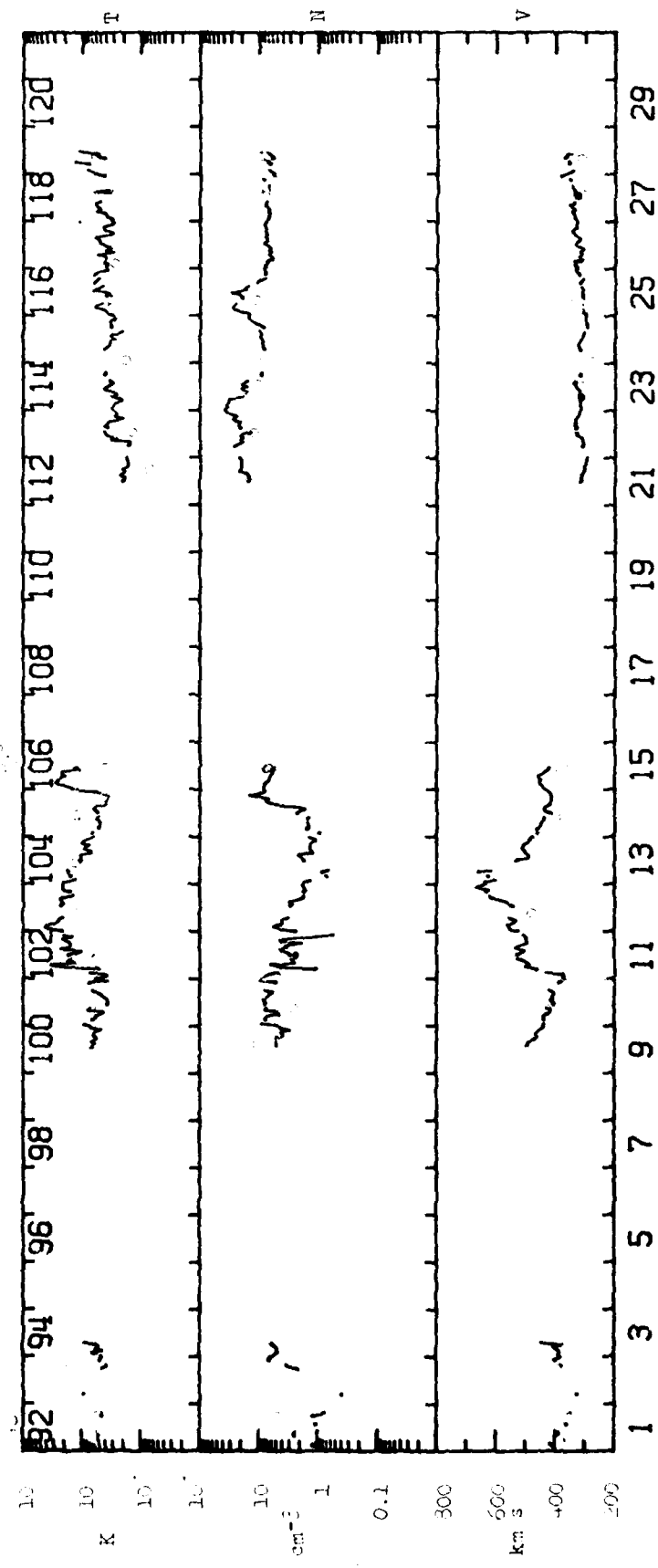


Figure 2d

130

Figure 3b

